

# Sacrificial bonds enhance toughness of dual polybutadiene networks

Barbara J. Gold<sup>a</sup>, Claas H. Hövelmann<sup>a\*</sup>, Christine Weiß<sup>a</sup>, Aurel Radulescu<sup>b</sup>, Jürgen Allgaier<sup>a</sup>,  
Wim Pyckhout-Hintzen<sup>a</sup>, Andreas Wischnewski<sup>a</sup>, Dieter Richter<sup>a</sup>

<sup>a</sup>*Jülich Centre for Neutron Science (JCNS-1) and Institute for Complex Systems (ICS-1), Forschungszentrum  
Jülich GmbH, 52425 Jülich, Germany*

<sup>b</sup>*Jülich Centre for Neutron Science (JCNS), Forschungszentrum Jülich GmbH, Outstation at MLZ,  
Lichtenbergstraße 1, 85747 Garching, Germany*

## Highlights

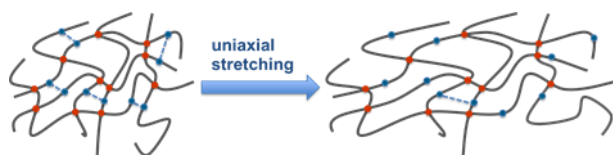
- Synthesis of permanent/transient dual polybutadiene networks
- No change in Gaussian chain conformation compared to linear chains proven by small angle neutron scattering
- Stress-strain measurements and Mooney-Rivlin analysis for mechanical characterization
- Enhanced mechanical properties result from transient sacrificial bonds

## Abstract

A new dual network elastomer is developed that consists of polybutadiene crosslinked with both permanent and transient bonds. The transient network is formed by the association of urazole groups that are randomly attached to the polymer backbone. Subsequent orthogonal covalent crosslinking through hydrosilylation in the melt state leads to a dual network with variable permanent and transient crosslinking density. Small angle neutron scattering (SANS) investigations show a homogeneous distribution of the transient bonds in both the functionalized polymers and the dual network products. The enhanced mechanical properties of the dual networks compared to conventional polybutadiene elastomers are characterized by stress-strain measurements. The increased

toughness can be explained by a protective mechanism where the weaker supramolecular bonds act as sacrificial bonds that dissipate energy.

### Graphical abstract



### Keywords

Dual network; Hydrogen bond; Polybutadiene

## 1. Introduction

Elastomers which consist of long polymer chains, crosslinked in a curing process, play an important role in multiple applications due to their unique physical properties like high flexibility and reversible deformation. They are widely used in the production of diverse materials like dampeners, seals, adhesives and tires. Since the discovery of the entropic nature of rubber elasticity [1] great efforts have been made to understand the physics of polymer network chains on the microscopic level. The first model that successfully described rubber elasticity in many aspects on a molecular basis is the phantom network model [2] which does not consider any topological interactions between the network chains. Several attempts to account for them [3,4] were made up to now. They differ in the treatment of chain entanglements and of crosslink fluctuation. Experimental studies [5] as well as computer simulations [6] evidence that one of the most successful topological theories to describe rubber elasticity are mean field tube models [7] like e.g. the Heinrich-Straube-Helmis [3] or the Panyukov-Rubinstein [8] model in which the contribution of the average tube confinement and crosslink dynamics enter naturally and describe the transition between the free fluctuating phantom models into the affine limit at small deformations. To increase the toughness of conventional elastomers several strategies have been developed in the last decades.

A recent approach is based on the addition of a second interpenetrating network with strongly different crosslinking density. This concept has been described first for structurally related hydrogels [9] and was recently applied in the synthesis of elastomers by Creton and Sijbesma [10]. Under deformation the stress in the network with the high crosslinking density increases faster and eventually leads to rupture of the chemical bonds, thereby dissipating energy. The higher elasticity of the second surviving network however allows for further reversible deformation. The disadvantage of these “sacrificial” bonds lies in the irreversibility of the energy dissipation process. Once the crosslinks in the first covalent network are destroyed, they cannot reform. The double network concept can be extended using transient, reversible bonds for the sacrificial network that should enable reversible energy dissipation [11]. In order to distinguish them from the aforementioned double networks and to emphasize the existence of two different kinds of crosslinks on each chain we will refer to them as dual networks [12]. A pioneering work by Schadebrodt et al. [13] describes the synthesis of a polybutadiene or NBR based networks containing isophthalic diamide groups. These are able to form three-dimensional hydrogen bonded aggregates which separate into thermo-reversible hard phases. The combination with covalent crosslinks results in “smart rubbers”, networks with transient and covalent crosslinks which exhibit temperature dependent mechanical properties. Other examples of dual networks can be found in hydrogels [14], small molecule based supramolecular polymers [15], shape-memory polymers [16], biopolymers [17], telechelic elastomers [18] and coating materials [19]. An alternative biomimetic approach by the Guan group uses extendable crosslinks that incorporate hydrogen bonds to mimic the muscle protein titin [20]. Dual crosslinked PIB star polymers with a low covalent crosslinking density were even shown to exhibit self-healing abilities [21]. In general, increased material strength and toughness is observed in dual networks compared to the corresponding conventional materials. Our work focuses on transferring the dual network concept to conventional elastomers by developing a well defined and predictable network architecture (figure 1). Controlling the chain length and the crosslinking density in both network types independently allows the production of dual networks tailored to meet specific physical criteria. Therefore we focus on model polydienes that already have a long history as elastomeric materials and can be synthesized with known microstructure and exact molecular weight, a requirement to relate the transient and permanent crosslink density per chain. In contrast to most known systems that base their transient crosslinks on strong hydrogen bonding motifs like 4-ureido-2-pyrimidone (UPy) [22] or three-dimensional aggregation we designed our dual network concept using weak directed supramolecular bonds to avoid secondary interactions like cluster formation, stacking or microphase separation. In the following we present a route that allows the independent adjustment of both permanent and transient crosslink density of a model polybutadiene. We show by

small angle neutron scattering that the incorporation of the hydrogen bond moieties does not lead to segregation of supramolecular groups [13,23] but preserves the Gaussian statistics of the backbone chains at all length scales. Furthermore, a mechanical characterization of pure and dual networks is discussed. In the context of this work and in view of the small strains that are achieved, the phenomenological theory of Mooney and Rivlin [24] was used to deliver a proof-of-principle of our dual network concept. We conclude that via replacing a certain amount of permanent crosslinks with reversible ones, the properties of elastomers can be enhanced significantly while the material strength remains unchanged.

## 2. Experimental

### 2.1. Synthesis

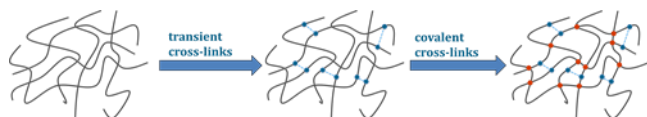
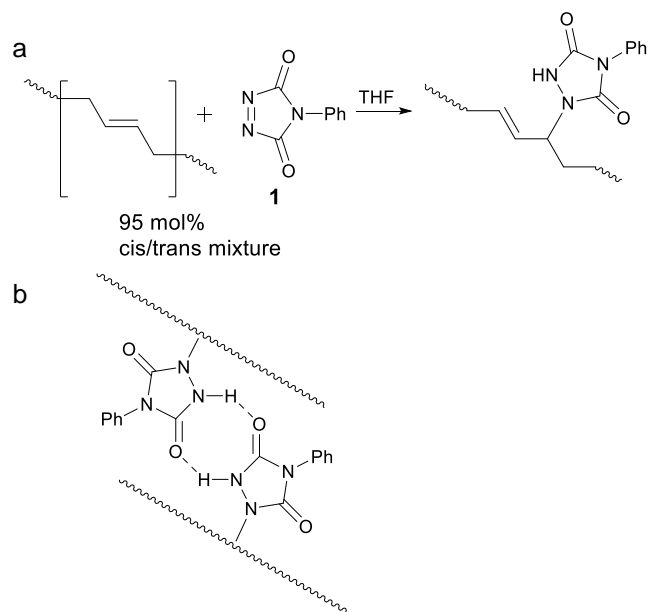


Figure 1. Stepwise formation of a dual elastomeric network.

For the formation of the first, transient network we used the known addition of 4-phenyl-1,2,4-triazoline-3,5-dione (**1**) to polydienes via Alder-ene reaction to form urazoles (scheme 1). This reaction was first described by Butler [25] and later extensively studied by the Stadler group [26]. Addition of **1** to polybutadiene in THF forms the functionalized polymer within minutes. The ene reaction of the triazoline proceeds chemoselectively with the internal double bonds of the polymer. The resulting materials show interaction of two urazole groups via the formation of two hydrogen bonds. These supramolecular crosslinks are homogeneously distributed throughout the material and no cluster formation could be observed [27]. In a subsequent covalent crosslinking step a Pt catalyzed hydrosilylation procedure with a bissilane crosslinker was used [28]. In contrast to established radical based crosslinking reactions hydrosilylation proceeds at lower temperatures and avoids scission of the polymer chains.

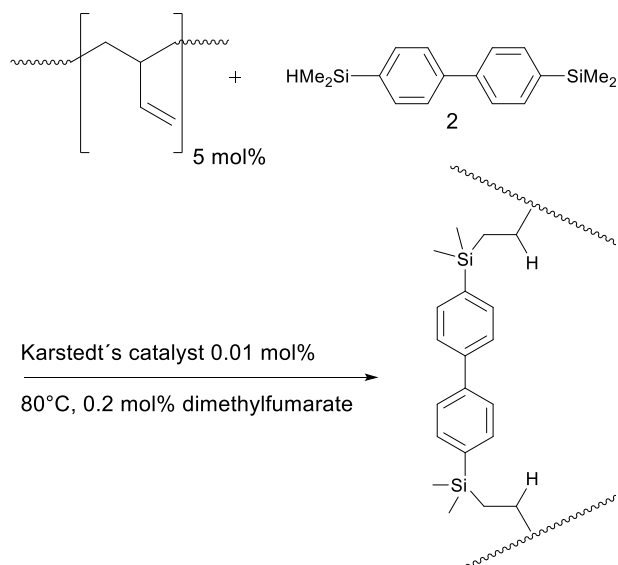
Scheme 1. Formation of urazole-based transient network.



a) formation of urazole-functionalized PB via ene reaction. b) formation of transient H-bond crosslinks.

Hydrosilylation crosslinking of polybutadiene proceeds mainly by reaction with the vinylic 1,2 moieties thereby using orthogonal reaction conditions to the urazole functionalization step. To achieve a homogeneous distribution of crosslinker and catalyst all reagents were mixed in solution. The resulting mixture was dried before curing in the melt state. Low molecular weight crosslinkers like 1,4-bis dimethylsilyl-benzene proved to be too volatile for this procedure and resulted in lower and inhomogeneous network densities.

Scheme 2. Covalent crosslinking.



The use of 4,4'-tetramethylbissilyl-biphenyl (**2**) in combination with Karstedt's catalyst (scheme 2) provides a crosslinker with low volatility that allows mixing of the reagents in solution followed by complete drying of the sample without loss of crosslinker. However, crosslinking by hydrosilylation led to premature reaction at room temperature during the sample preparation. This was avoided by addition of 0.2 mol% dimethylfumarate as inhibitor to raise the effective crosslinking temperature to 80 °C [29]. A solution NMR study showed only a negligible effect of the added dimethylfumarate on the association of the urazole dimers (see supporting information). The final crosslinking reaction was conducted in a Teflon mold under an argon atmosphere to form 20 mm x 20 mm x 1 mm elastomer samples. To ensure that the urazole crosslinks are not inversely affected by the curing procedure both the transient and dual networks were investigated by IR spectroscopy. The absorption of the urazole groups in the carbonyl region provides detailed information about the state of the hydrogen bonds and has been previously used to determine the association constant of the transient bonds in a polymer melt [30]. No change in IR absorption could be observed between the transient and the dual network [31]. Three samples of covalent and dual networks were synthesized from anionically polymerized polybutadiene ( $M_w = 60$  kg/mol). N1 and N2 have a covalent crosslinking density of 0.5 mol% and 1 mol% of monomeric units. N3 is a dual network

consisting of 0.5 mol% permanent crosslinks and 2 mol% urazole functionalization. Assuming initially full conversion in the covalent crosslinking reaction and equidistant placing the number of crosslinks per chain  $N_c$  and the average molecular weight (mesh size) between covalent crosslinks  $M_c$  amounts to  $N_c = 5.5$ ,  $M_c = 9.2$  kg/mol for N1 and N3 and  $N_c = 11$ ,  $M_c = 5.0$  kg/mol for N2 using the following relations

$$N_c = \frac{M_w}{M_0} x_{cov} \quad (1)$$

$$M_c = \frac{M_w}{N_c + 1} \quad (2)$$

where  $M_0 = 54.09$  g/mol is the molar mass of polybutadiene monomer and  $x_{cov}$  is the molar fraction of covalent crosslinks.

## 2.2. Determination of crosslinking efficiency via swelling experiments

The efficiency of crosslinking was checked via equilibrium swelling measurements in a good solvent (cyclohexane) from which the mesh size  $M_{c,swell}$  can be determined experimentally. Three independent swelling experiments for sample N2 (covalent network, crosslink density 1 mol%) were carried out.  $M_{c,swell}$  was calculated according to equation 3, which takes into account dangling chain ends, and compared with its theoretical value  $M_c$ .

$$\frac{-(\ln(1-Q^{-1}) + Q^{-1} + \chi Q^{-2})}{V_{mol,cyclo} (Q^{-1/3} - 0.5 Q^{-1})} + \frac{\rho_{PB}}{M_w} = \frac{\rho_{PB}}{M_{c,swell}} \quad (3)$$

$$Q = \left( \frac{m_{swollen}}{m_{dried}} - 1 \right) \frac{\rho_{PB}}{\rho_{cyclo}} + 1 \quad (4)$$

Equation 4 represents the swelling degree  $Q$  where  $\rho_{PB} = 0.895$  g/cm<sup>3</sup> is the density of PB [32],  $\rho_{cyclo} = 0.779$  g/cm<sup>3</sup> the density of cyclohexane,  $V_{mol,cyclo} = 107.8$  cm<sup>3</sup>/mol the molar volume of cyclohexane and  $\chi = 0.21$  the Flory-Huggins polymer solvent interaction parameter [33]. The results of the swelling tests are summarized in table 1.

**Table 1. Characterization by swelling.**

swelling	test 1	test 2	test 3
Q	6.8	6.9	6.7
$M_{c,swell}$ [g/mol]	5310	5460	5150

The average experimental mesh size amounts to  $M_{c,swell} = 5300 \pm 200$  g/mol which leads to an effective conversion for the covalent crosslinking reaction of  $94 \pm 4$  % compared to its theoretical value  $M_c = 5000$  g/mol.

### 3. Results and Discussion

#### 3.1 Study of chain conformation via small angle neutron scattering (SANS)

To exclude phase separation or clustering of the functional groups, the conformation of the backbone chains with and without urazole has been investigated at 298 K via SANS. To provide the necessary contrast 5 m% of hydrogenous polybutadiene was replaced by its deuterated analog. The hydrogenous and deuterated polymers were mixed via solution blending in tetrahydrofuran before functionalization. The SANS measurements were carried out at the KWS-2 at MLZ, Garching, Germany. A neutron wavelength of  $\lambda = 5$  Å and sample-to-detector distances of  $d = 2$  m, 8 m and 20 m were used to cover a broad scattering vector  $Q$  between  $10^{-3}$  Å<sup>-1</sup> to 0.15 Å<sup>-1</sup>. The scattering intensity was detected via a two-dimensional scintillation detector with a resolution of 128 x 128 pixels and a pixel size of 5 x 5 mm<sup>2</sup> each. Data were radially averaged, merged and corrected for background scattering and transmission. By calibration with a plexiglass standard absolute scattering intensities were obtained. **Figure 2** presents coherent SANS data at ambient T in a Kratky representation. This representation which bases on the Debye scattering function of an undisturbed Gaussian chain was chosen as a most sensitive approach to compare chain conformations at different stages of the dual network synthesis. It highlights the random walk behavior of the base polymer which should be strongly disturbed if the functional groups would cluster or segregate. As can be seen from **figure 2**, the scattering intensities from the pure linear, urazole-functionalized, covalent network and dual network system all plateau in the same region which shows that they are all Gaussian coils and chain dimensions are preserved in each step towards the dual networks.



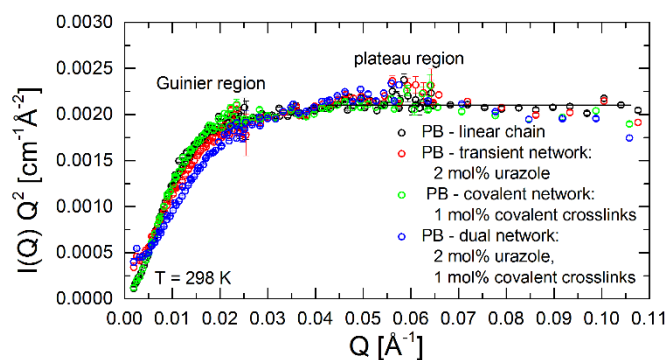


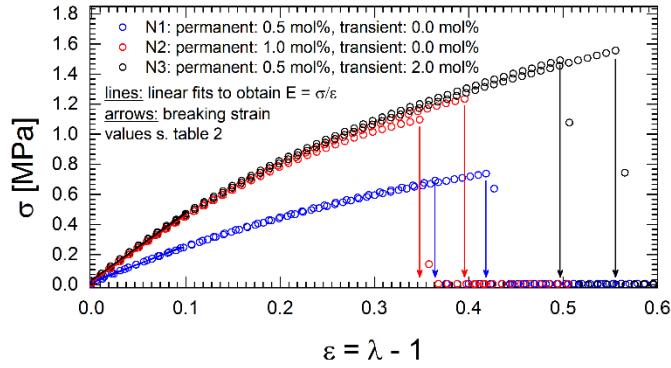
Figure 2. Kratky (2<sup>nd</sup> moment) representation of scattering intensities at each step towards the corresponding dual network synthesis.

No change in the Gaussian chain conformation or of the coil size of the chains could be detected. In contrast to previous SANS experiments on systems with large three-dimensional aggregates in polybutadiene [23], where the Q-range was limited to the Guinier region, we proved Gaussian chain structures at all length scales.

### 3.2. Stress-Strain investigation

To investigate the influence of the additional transient crosslinks on the mechanical properties of polybutadiene dual networks uniaxial stress-strain measurements have been performed at  $T = 298$  K. The strain was increased linearly with a crosshead speed of 0.1 mm/s. Specimens with a minimum length-to-width ration of 4:1 and a thickness of 1 mm were cut out from the network sheets and clamped horizontally with an initial gauge length of 10 mm between the jaws of an rheometer (ARES, Rheometric Scientific, Inc.) equipped with a 2K-FRT transducer. The exact undeformed measures of the specimen was measured with a digital vernier caliper (precision 0.02 mm). The engineering stress-strain curves for the investigated networks N1, N2 and N3 are shown in figure 3.

a



b

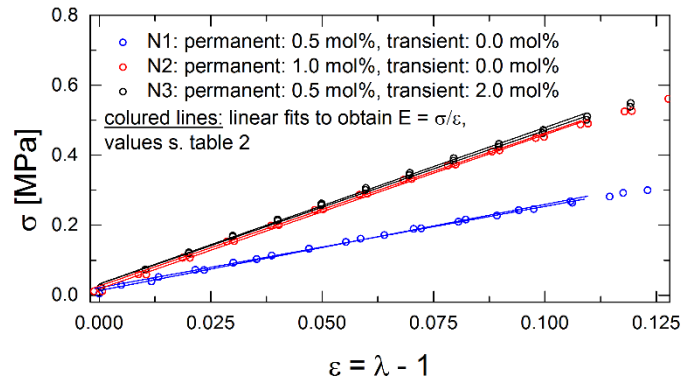


Figure 3. Engineering stress  $\sigma$  versus engineering strain  $\varepsilon = \lambda - 1$  with  $\lambda = L/L_0$  where  $L_0$  is the initial length of the sample between the clamps. Two measurements of each sample are shown. Arithmetic means of maximum extension  $\varepsilon_{\max}$  and Young's modulus  $E$  for each network are listed in table 2. a) breaking strain  $\varepsilon_{\max}$ . b) linear fits to obtain Young's modulus  $E$ .

From the small deformation limit ( $\lambda \leq 1.1$ ) Young's modulus  $E$  amounts to 2.4 MPa for a permanent crosslinking density of 0.5 mol% (N1). By doubling the permanent crosslinking degree to 1 mol% (N2) its value increases to 4.4 MPa. The same effect is achieved by a combination of 0.5 mol% covalent and 2 mol% transient crosslinks instead which leads to a Young's modulus of 4.5 MPa (N3). Although sample N2 and N3 show the same Young's modulus, the pure covalent network N2 ruptures at higher deformations at an extension of 37% while the dual network N3 withstands elongations up to 56%. A deeper insight into the influence of the covalent and transient crosslinks on the stress-strain response of the network samples can be achieved by the phenomenological Mooney-Rivlin analysis.

Within this phenomenological model [34] uniaxial stress-strain data can be described in good accuracy with

$$\sigma^*(\lambda) = \frac{\sigma(\lambda)}{\lambda - \frac{1}{\lambda^2}} = 2C_1 + 2C_2 \frac{1}{\lambda} \quad (5)$$

where  $\sigma(\lambda)$  is the engineering and  $\sigma^*(\lambda)$  is the reduced engineering stress. Therewith, the initial modulus of the network is given as

$$G_0 \equiv \lim_{\lambda \rightarrow 1} \sigma^* = 2C_1 + 2C_2 \quad (6)$$

At small deformations and assuming a Poisson's ratio of 0.5 as for ideal rubbers, the initial shear modulus  $G_0$  and the corresponding Young's modulus  $E_{MR}$  can be calculated from the Mooney-Rivlin constants  $2C_1$  and  $2C_2$  as follows:

$$3G_0 = E_{MR} = 3(2C_1 + 2C_2) \quad (7)$$

On the other hand in equation 5 the limit of  $\lambda \rightarrow \infty$  yields  $\sigma^*(\lambda) = 2C_1$ . Since topology and/or transient links vanish then,  $2C_1$  represents the contribution of the permanent chemical crosslinks to the total modulus [35]. Likewise  $2C_2$  contains all contributions of topological/transient interactions between the network chains [36]. Assuming affine deformation the mesh size  $M_{C-MR}$  can be calculated from the Mooney-Rivlin constant  $2C_1$  with the following relation [37]

$$M_{C-MR} = \frac{\rho_{PB} R T}{2C_1} \quad (8)$$

where  $\rho_{PB} = 0.895 \text{ g/cm}^3$  [32] is the density of polybutadiene,  $R$  the gas constant and  $T = 298 \text{ K}$  the measurement temperature. In figure 4 the Mooney-Rivlin analysis of network samples N1, N2 and N3 is shown. The obtained values of  $2C_1$  and  $2C_2$  are given in table 2. These moduli are extremely sensitive to the fit range, which is limited in the case of polybutadiene, as well as small errors in the initial length of the test specimen [38] what leads after a thorough error estimation to an uncertainty of around 20 % in our case.

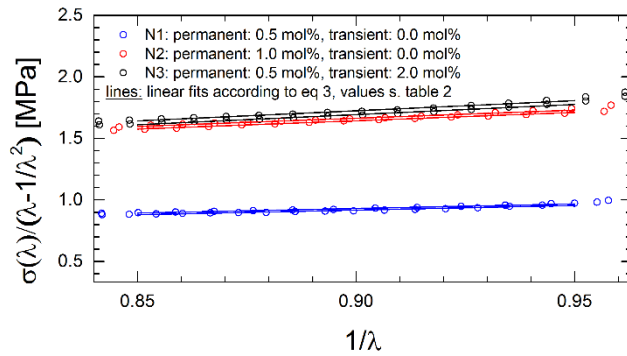


Figure 4. Mooney-Rivlin representation of uniaxial stress-strain data. Lines represent linear fits according to equation 5. The arithmetic means of the resulting Mooney-Rivlin constants  $2C_1$  and  $2C_2$  are listed in table 2.

A comparison between the values of  $M_c$ ,  $M_{c,swell}$  and  $M_{c-MR}$  as well as  $E$  and  $E_{MR}$  and the values of the moduli  $G_0$  are listed in table 2. The fitted Young's modulus  $E$  and the Young's modulus  $E_{MR}$  calculated from the Mooney-Rivlin constants are in good agreement within their error tolerances. In contrast to the Young's modulus from the small deformation limit, the Mooney-Rivlin analysis in principle allows to decompose the overall modulus into its components. The comparison of  $2C_1$  for the different samples shows clearly that this constant reflects the pure affine contribution of the chemical network. For N1 and N3 both having a covalent crosslinking density of 0.5 mol% the values of  $2C_1$  are identical but double for sample N2 which has a double covalent crosslinking density of 1 mol%. The resulting average mesh size  $M_{c-MR}$  calculated from the Mooney-Rivlin parameter  $2C_1$  is in very good agreement with  $M_{c,swell}$  for network N2 and  $M_c$  for all networks. Therefore it can be concluded that the use of the bishydrosilane crosslinker has a almost 100 % reaction efficiency, as also shown from the swelling experiments, and most importantly is not influenced by the urazole groups. In similar studies on pure covalent polybutadiene networks with comparable covalent crosslink densities and microstructure a maximal elongation of 25 % to 40 % is reported [38], which we also observe for the covalent network samples N1 and N2. With the identical amount of covalent crosslinks for N1 and N3 the reproducible enhanced elongation up to 56 % of the dual network N3 emphasizes that the increased toughness of the dual network samples results entirely from the additional transient crosslinks. During the application of mechanical stress the rubber strands becomes strained and mechanical forces act on both types of crosslinks. By opening the transient crosslinks excess stress is released and the strand is able to relax locally. This stress relief mechanism results in a higher maximum

elongation of the dual network N3 compared to the pure covalent sample N1. Subsequent re-association of the transient crosslinks leads to recovered mechanical strength in a more stress free state.

**Table 2. Permanent and transient crosslinking density, maximum elongation  $\epsilon_{\max}$ , Mooney-Rivlin constants and moduli for networks N<sub>1</sub>, N<sub>2</sub> and N<sub>3</sub>**

sample	N <sub>1</sub>	N <sub>2</sub>	N <sub>3</sub>
perm cld [mol%]	0.50	1.0	0.50
trans cld [mol%]	-	-	2.0
$\epsilon_{\max}$	0.39 $\pm$ 0.027	0.37 $\pm$ 0.024	0.53 $\pm$ 0.029
2C <sub>1</sub> [MPa]	0.23 $\pm$ 0.047	0.44 $\pm$ 0.087	0.23 $\pm$ 0.045
2C <sub>2</sub> [MPa]	0.77 $\pm$ 0.15	1.4 $\pm$ 0.27	1.6 $\pm$ 0.33
G <sub>0</sub> [MPa]	1.0 $\pm$ 0.20	1.8 $\pm$ 0.36	1.8 $\pm$ 0.38
E <sub>MR</sub> [MPa]	3.0 $\pm$ 0.60	5.4 $\pm$ 1.1	5.4 $\pm$ 1.1
E [MPa]	2.4 $\pm$ 0.1	4.4 $\pm$ 0.1	4.5 $\pm$ 0.1
M <sub>c</sub> [kg/mol]	9.2	5.0	9.2
M <sub>c-MR</sub> [kg/mol]	10 $\pm$ 2.0	5.2 $\pm$ 1.0	10 $\pm$ 2.0
M <sub>c,swell</sub>	-	5.3 $\pm$ 0.2	-

### 3.2. Linear shear rheology

The suggested stress-relief mechanism at moderate strain has its counterpart in the linear rheological behavior. To investigate the relaxation process of the transient groups, shear rheology measurements were carried out on functionalized polybutadiene with 2 mol% urazole groups and a reference system of pure linear polybutadiene. For this purpose the same rheometer as for the stress-strain investigations was used. Linear rheology data were obtained in plate-plate geometry (diameter 8 mm). Oscillatory shear measurements from  $\omega = 0.1$  rad/s to  $\omega = 100$  rad/s were recorded from T = 193 K to T = 343 K using a temperature interval of  $\Delta T = 15$  K and a strain of  $\gamma = 1$

% to stay in the linear regime. Via applying the time-temperature-superposition principle as described for urazole-functionalized systems by Stadler [39] mastercurves for the reference temperature  $T_{\text{ref}} = 298 \text{ K}$  were created (figure 5b). The corresponding horizontal shift factors  $a_T$  which show a WLF behavior are demonstrated in figure 5a where also the corresponding empirical WLF parameter  $C1$  and  $C2$  are reported.

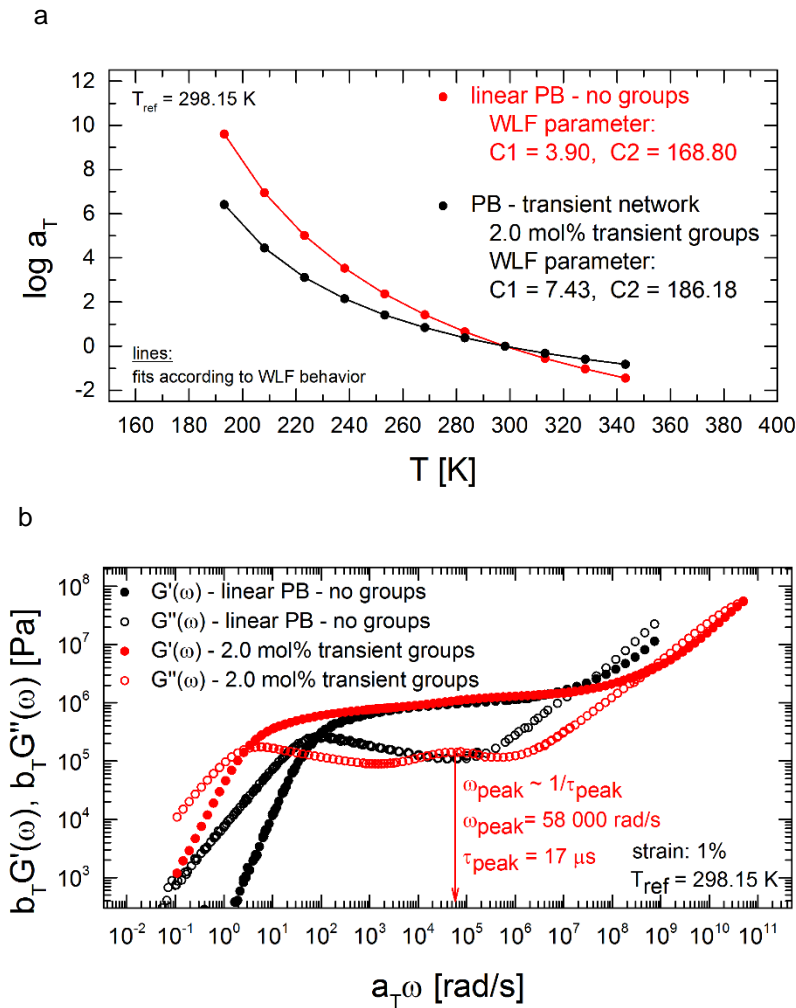


Figure 5. Linear shear rheology for linear (unfunctionalized) and urazole-functionalized PB. a) horizontal shift factors and WLF parameter corresponding to  $T_{\text{ref}} = 298.15 \text{ K}$ . b) dynamic storage and loss moduli. A clear second relaxation process due to the functional groups is observed.

Besides a slowing down of the chain dynamics, the functional groups lead to a pronounced second relaxation process in the dynamic loss modulus at a frequency of  $58 \cdot 10^3 \text{ rad/s}$  corresponding to a characteristic time of  $\tau = 17 \text{ }\mu\text{s}$ . In the storage modulus a drop is observed at the same frequency. Based on the sticky reptation model of

Leibler, Rubinstein and Colby [40], in which the stress relaxation modulus of a thermoreversible network is described theoretically, this second relaxation process is correlated to the lifetime of the temporary junctions. Therefore, it provides evidence that the suggested stress-relief mechanism in the dual network is induced by the very fast opening and re-association of the functional groups.

#### **4. Conclusion**

In conclusion we demonstrate the synthesis of a well-defined polybutadiene dual network based on a reaction sequence of urazole functionalization and a hydrosilylation curing step. Both reactions use orthogonal reaction conditions and allow for the independent adjustment of the transient and permanent crosslinking density. No change in the Gaussian chain conformation could be observed due to synthesis. Stress-strain investigations show enhanced mechanical and ultimate properties of the dual network samples due to the sacrificial transient crosslinks in the system compared to conventional rubbers with the same amount of covalent crosslinks. We claim that this effect is related to the opening and recombination of the functional groups, as a second relaxation process occurs for the urazole-functionalized system in linear shear rheology measurements. The mechanism is general and will be observed for all polydienes. Polybutadiene having a low molecular entanglement weight suffers from a relatively restricted elongation [38] as the number of entanglements is equal or higher than the crosslinking density of the network. This situation is relieved for less entangled and more rubbery polydienes like polyisoprene or natural rubbers that allow stronger deformations. Therefore, we based our further more detailed studies of the protective mechanism in dual networks on polyisoprene as base polymer. These investigations will be published elsewhere in combination with extensive static and dynamic neutron scattering analyses.

#### **ASSOCIATED CONTENT**

Supporting Information. All experimental details including sample preparation and characterization.

#### **AUTHOR INFORMATION**

Corresponding Author

\*E-mail: c.hoevelmann@fz-juelich.de Tel.: +49-2461-61 5022.

## Notes

The Authors declare no competing financial interest.\*

## ACKNOWLEDGMENT

C. W. acknowledges financial support by the European Community's 7th Framework Programme under grant agreement no.309450 SHINE. We thank Dr. L. Willner for providing the deuterated polybutadiene for the SANS studies.

## REFERENCES



- [1] (a) Gough J. *Mem. Lit. Phil. Soc. Manchester* 1805; 1: 288-295. (b) Joule P. *Phil. Trans. R. Soc. London A* 1859; 149: 91-131. (c) Thomson W. *Quart. J. Math.* 1857; 1: 55-77.
- [2] (a) James HM. *Chem. Phys.* 1947; 15: 651-668. (b) James HM, Guth E. *J. Chem. Phys.* 1948; 11: 455-481. (c) Flory PJ. *Proc. R. Soc. London A* 1986; 351: 351-380. (d) Higgs PG, Ball RC. *J. Phys. France* 1988; 49: 1785-1811. (e) Rubinstein M, Panyukov SV. *Macromolecules* 1997; 30: 8036-8044.
- [3] Heinrich S, Straube E, Helms G. *Adv. Pol. Sci.* 1988; 85: 34-87.
- [4] Rubinstein M, Panyukov S. *Macromolecules* 2002; 35: 6670-6686.
- [5] (a) Straube E, Urban V, Pyckhout-Hintzen W, Richter D, Glinka CJ. *Phys. Rev. Lett.* 1995; 74: 4464-4467. (b) Westermann S, Urban V, Pyckhout-Hintzen W, Richter D, Straube E. *Macromolecules* 1996; 29: 6165-6174.
- [6] (a) Everaers R. *New J. Phys.* 1999; 1: 12.1-12.54. (b) Duering ER, Kremer K, Grest GS. *Phys. Rev. Lett.* 1991; 67: 3531-3534. (c) Duering ER, Kremer K, Grest GS. *J. Chem. Phys.* 1994; 101: 8169-8192. (d) Everaers R, Kremer K. *Macromolecules* 1995; 28: 7291-7294.
- [7] (a) Edwards SF. *Proc. Phys. Soc.* 1967; 92: 9-16. (b) Rubinstein M, Panyukov S. *Macromolecules* 1997; 30: 8036-8044. (c) Edwards SF, Vilgis TA. *Rep. Prog. Phys.* 1988; 51: 243-297. (d) Doi M. *J. Polym. Sci., Polym. Lett. Ed.* 1981; 19: 265-271.
- [8] Rubinstein M, Panyukov S. *Macromolecules* 2002; 35: 6670-6686
- [9] (a) Gong JP, Katsuyama Y, Kurokawa T, Osada Y. *Adv. Mater.* 2003; 15: 1155-1158. (b) Yu QM, Tanaka Y, Furukawa H, Kurokawa T, Gong JP. *Macromolecules* 2009; 42: 3852-3855.
- [10] Ducrot E, Chen Y, Bulters M, Sijbesma RP, Creton C. *Science* 2014; 344: 186-189.
- [11] Wijtecki RJ, Meador MA, Rowan SJ. *Nature Mater.* 2011; 10: 14-27.
- [12] Fajardo AR, Fávoro SL, Rubira AF, Muniz CE. *React. Funct. Polym.* 2013; 73: 1662-1671.
- [13] Schadebrodt J, Ludwig S, Abetz V, Stadler R. *Kautschuk Gummi Kunststoffe* 1999; 52: 555-564.
- [14] (a) Sun JY, Zhao X, Illeperuma WRK, Chaudhuri W, Hwan Oh K, Mooney DJ, Vlassak JJ, Suo Z. *Nature* 2012; 489: 133-136. (b) Mayumi K, Marcellan A, Ducouret G, Creton C, Narita T. *ACS Macro Lett.* 2013; 2: 1065-1068.
- [15] (a) Montarnal D, Cordier P, Soulié-Ziakovic C, Tournilhac F, Leibler L. *J. Polym. Sci., Part A: Polym. Chem.* 2008; 46: 7925-7936. (b) Montarnal D, Tournilhac F, Hidalgo M, Couturier JL, Leibler L. *J. Am. Chem. Soc.* 2009; 131: 7966-7967. (c) Montarnal D, Tournilhac F, Hidalgo M, Leibler L. *J. Polym. Sci., Part A: Polym. Chem.* 2010; 48: 1133-1141.
- [16] (a) Li J, Viveros JA, Wrue MH, Anthamatten M. *Adv. Mater.* 2007; 19: 2851-2855. (b) Li J, Lewis CL, Chen DL, Anthamatten M. *Macromolecules* 2011; 44: 5336-5343. (c) Ware T, Hearon K, Lonneckner A, Wooley KL, Maitland DJ, Voit W. *Macromolecules* 2012; 45: 1062-1069.
- [17] Skrzyszewska PJ, Jong LN, de Wolf FA, Cohen Stuart MA, van der Gucht J. *Biomacromolecules* 2011; 12: 2285-2292.
- [18] (a) Monemian S, Jang KS, Ghassemi H, Korley LTJ. *Macromolecules* 2014; 47: 5633-5642. (b) Kumpfer JR, Rowan SJ. *J. Am. Chem. Soc.* 2011; 133: 12866-12874.
- [19] Wietor JL, Dimopoulos A, Govaert LE, van Benthem RATM, de With G, Sijbesma RP. *Macromolecules* 2009; 42: 6640-6646.
- [20] (a) Kushner AM, Gabuchian V, Johnson EG, Guan Z. *J. Am. Chem. Soc.* 2007; 129: 14110-14111. (b) Schuetz J-H, Peng W, Vana P. *Polym. Chem.* 2015; 6: 1714-1726.
- [21] Döhler D, Peterlik H, Binder WH. *Polymer* 2015; 69: 264-273.
- [22] Sijbesma RP, Beijer FH, Brunsveld L, Folmer BJB, Hirschberg JHKK, Lange RFM, Lowe JKL, Meijer EW. *Science* 1997; 278: 1601-1604.
- [23] Abetz V, Dardin A, Stadler R, Hellmann J, Samulski ET, Spiess H-W. *Colloid Polym. Sci.* 1996; 274: 723-731
- [24] (a) Mooney MJ. *Appl. Phys.* 1940; 11: 582-592. (b) Rivlin RS. *J. Appl. Phys.* 1948; 18: 444-449.
- [25] Butler GB. *Ind. Eng. Chem. Prod. Res. Dev.* 1980; 19: 512-528.
- [26] (a) Stadler R, Burgert J. *Makromol. Chem.* 1986; 187: 1681-1690. (b) Stadler R, de Lucca Freitas L. *Colloid Polym. Sci.* 1986; 264: 773-778.
- [27] Stadler R, Burgert J, de Lucca Freitas L. *Polym. Bull.* 1987; 17: 431-438.
- [28] (a) Friedmann G, Hem J, Brossas J. *Polym. Bull.* 1982; 6: 251-257. (b) Aranguren MI, Macosko CW. *Macromolecules* 1988; 21: 2484-2491.
- [29] Lewis LN, Stein J, Colborn RE, Gao Y, Dong JJ. *Organomet. Chem.* 1996; 521: 221-227.
- [30] (a) Stadler R, de Lucca Freitas L. *Polym. Bull.* 1986; 15: 173-179. (b) de Lucca Freitas L, Auschra C, Abetz V, Stadler R. *Colloid Polym. Sci.* 1991; 269: 566-575.
- [31] see supporting information
- [32] Fetters LJ, Lohse DJ, Richter D, Witten TA, Zirkel A. *Macromolecules* 1994; 27(17): 4639-4647.
- [33] Lau WR, Glover CJ, Holste JC. *J. Appl. Polym. Sci.* 1982; 27: 3067-3077.
- [34] (a) Mooney MJ. *Appl. Phys.* 1940; 11: 582. (b) Rivlin RSJ. *Phil. Trans. R. Soc. London A* 1948; 240: 459-490.
- [35] Mark JE. *Rubber Chem. Technol.* 1975; 48: 495-512.
- [36] Ferry JD. *Viscoelastic Properties of Polymers*, John Wiley & Sons, New York 1980 (3rd edition).
- [37] Mark JE, Erman B. *Rubberlike Elasticity: A Molecular Primer*, John Wiley & Sons, New York 1988.
- [38] Dossin LM, Graessley WW. *Macromolecules* 1997; 12(1): 124-130.
- [39] de Lucca Freitas L, Stadler R. *Colloid Polym. Sci.* 1988; 266: 1095-1101.
- [40] Leibler L, Rubinstein M, Colby RH. *Macromolecules* 1991; 24: 4701-4707.